

A Multi-Hop Routing Solution for Low Latency and Energy Efficiency in Large-Scale LoRa IoT

M. Misbahuddin, M. S. Iqbal, L. A. S. Irfan Akbar

Misbahuddin Misbahuddin*

Department of Electrical Engineering, Faculty of Engineering,
University of Mataram, Mataram, 83125, Indonesia

*Corresponding author: misbahuddin@unram.ac.id

Muhamad Syamsu Iqbal

Department of Electrical Engineering, Faculty of Engineering,
University of Mataram, Mataram, 83125, Indonesia

msiqbal@unram.ac.id

Lalu Ahmad Syamsul Irfan Akbar

Department of Electrical Engineering, Faculty of Engineering,
University of Mataram, Mataram, 83125, Indonesia

irfan@unram.ac.id

Abstract

This paper presents a novel multi-hop routing approach for large-scale LoRa IoT networks that aims to solve the challenges of low latency and energy efficiency. The proposed protocol seeks to minimize energy usage and enable wirelessly data transfer by utilizing the unique features of LoRa communication technology. To ensure reliable communication in a multi-hop context, the protocol includes a dynamic routing mechanism that optimizes network latency and prevents data packet collisions. Furthermore, scalability is another important consideration since it permits the flexible addition of new nodes. The simulation results show that the proposed approach is effective, which shows improved energy savings, less latency, and strong flexibility. These results offer a promising solution for optimizing the performance of large-scale LoRa IoT deployments.

Keywords: multi-hop routing, low latency, energy efficiency, large-scale LoRa IoT.

1 Introduction

A recent development in Internet of Things (IoT) networks, LoRa is designed to transmit data over distances significantly greater than traditional wireless technologies in low energy, allowing devices to operate on low power, making it ideal for IoT applications requiring extended coverage, such as smart cities [1], agriculture [2], healthcare [3], and industrial monitoring & automation [4], etc. This characteristic is crucial for battery-operated devices in IoT applications, where minimizing

power consumption is essential for prolonged device lifetimes and remote deployments without frequent battery replacements [5]. The other advantage is that LoRa technology is well-suited for IoT environments, where a large number of devices need to communicate wirelessly to connect a wide range of IoT devices, including sensors, actuators, and other low-power devices that form the backbone of IoT networks. Moreover, LoRa offers a cost-effective solution for deploying large-scale IoT networks. Its long-range capabilities reduce the need for a dense network of base stations, leading to cost savings in infrastructure deployment. This makes LoRa an attractive option for IoT applications with widespread device deployment requirements. LoRa operates in unlicensed spectrum bands, providing flexibility and adaptability to various regulatory environments globally. This enables seamless deployment across different regions without the constraints associated with licensed spectrum technologies. LoRa is designed to perform well in challenging radio frequency conditions, including environments with obstacles and interference. This robustness enhances the reliability of communication, making it suitable for outdoor and industrial applications where signal quality can be affected by obstacles and interference.

The wireless network has two types of topology [6]: single-hop and multi-hop. The fundamental difference between single-hop and multi-hop communication in wireless networks lies in the number of intermediate nodes involved in transmitting data from the source to the destination. In a single-hop communication model, data travels directly from the source node to the destination node without involving any intermediate nodes. Whereas in a multi-hop communication model, data is relayed through multiple intermediate nodes to reach the destination node. The single-hop communication has advantages in typically simpler, with lower latency, and as data travels through a direct route, but it is constrained by the range limitations of the wireless technology, as the source and destination nodes need to be within direct communication range of each other. Whereas the multi-hop communication has advantages in extending the effective range of the network by allowing nodes beyond the direct range to participate in the communication, it can introduce higher latency due to the additional hops, and the complexity of routing algorithms and managing interference increases.

Multi-hop communication is necessary to transmit packets in some situations, such as industrial settings, agricultural settings, and subterranean tunnels, due to its advantages. There are two types of multi-hop LoRa-IoT topologies: multi-hop based on LoRaWAN and multi-hop based on LoRa. LoRa is a physical layer technology enabling long-range communication, whereas LoRaWAN is MAC layers that builds on top of LoRa to provide a network protocol with features like multi-hop communication, security, and network management for scalable IoT deployments. LoRaWAN is a better option if we need to provide an IoT device network that is multi-hop, managed, and secure. On the other hand, LoRa without the LoRaWAN protocol can be adequate if the application only needs basic point-to-point communication. This study investigates the use of deeper multi-hop communication to improve energy efficiency and latency in large-scale LoRa-IoT networks using the multi-hop network based on LoRa.

Figure 1 illustrates the both of topologies. An intermediate gateway is required in a multi-hop network based on LoRaWAN [7] - [13] to gather data from several end nodes and send packets to the main gateway, which will then forward them to the network server. On the other hand, a relay node is required as an intermediary to forward packets to the gateway in a multi-hop network based on LoRa [14] - [23].

LoRa is designed to perform well in challenging radio frequency conditions, including environments with obstacles and interference. This robustness enhances the reliability of communication, making it suitable for outdoor and industrial applications where signal quality can be affected by obstacles and interference. However, as the scale of LoRa-based IoT networks grows, several significant challenges emerge.

One of the primary challenges is energy efficiency in large-scale multi-hop LoRa networks [24] - [25]. LoRa devices typically operate on batteries, making efficient energy usage essential to prolong the lifetime of devices, especially in remote or difficult-to-access areas where regular battery replacement is impractical. While multi-hop communication can extend the range of LoRa networks, it tends to increase energy consumption as each node must relay data across multiple hops.

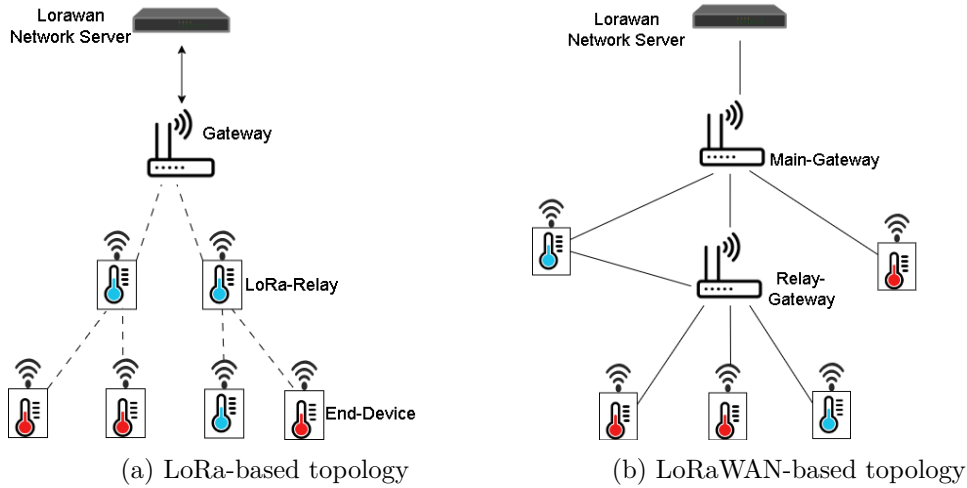


Figure 1: Topologies of multi-hop communication

Another challenge is latency in large-scale LoRa multi-hop networks [19]. Although multi-hop allows for extended range, each additional hop introduces delays in data transmission, potentially hindering applications that require fast response times or real-time communication, such as industrial monitoring and healthcare. High latency can reduce network responsiveness and delay critical data transmissions.

Finally, scalability poses a substantial challenge for multi-hop LoRa networks with numerous devices [26] - [27]. As the network scales, the growing number of devices can lead to communication bottlenecks and increased interference, potentially disrupting data transmission quality. Managing efficient communication paths in this environment requires a protocol that balances energy usage, maintains low latency, and supports network scalability.

In addressing these issues, this study proposes a novel multi-hop routing approach that optimizes energy efficiency and reduces latency in large-scale LoRa IoT networks without compromising scalability.

The key contributions of this paper are as follows: (i) overcoming the challenge of reducing communication delays in large-scale LoRa-IoT networks, (ii) improving network responsiveness by ensuring that packets can efficiently pass through multiple nodes, thus reducing latency between devices, (iii) minimizing energy consumption across large-scale LoRa IoT networks, (iv) enhancing energy efficiency to potentially extend the lifespan of battery-powered IoT devices, and (v) addressing scalability challenges inherent in large-scale LoRa IoT networks.

To achieve these objectives, this paper is structured as follows: Section 2 covers the related work, providing a comprehensive background for the proposed approach. Section 3 introduces the low-latency, energy-efficient multi-hop routing protocol. Section 4 presents a simulative assessment of the multi-hop approach based on LoRa and discusses the results obtained. Finally, Section 5 concludes the paper and suggests directions for future research.

2 Related Works

Several studies have explored multi-hop communication solutions that operate directly on the physical layer of LoRa, without involving the higher LoRaWAN protocol. These approaches aim to enhance the efficiency and performance of LoRa networks across various IoT applications. For example, [15] introduces a concurrent transmission technique that enables multiple nodes to transmit data simultaneously, improving the efficiency and throughput of multi-hop communication while addressing interference issues. This innovative approach significantly enhances network performance, though a limitation of this technique is that it can only be applied in a linear network, lacking flexibility for branch-like structures at the parent node.

In a different approach, [16] investigates the integration of the Routing Protocol for Low-power and Lossy Networks (RPL) into LoRa networks to improve multi-hop communication. RPL, designed

for low-power applications, addresses key challenges such as long-range communication and energy efficiency in LoRa networks. The protocol's ability to enable communication across multiple hops while conserving energy makes it highly suitable for IoT applications. However, the study's limitation lies in its focus on network connectivity rather than energy optimization, which could affect large-scale deployments.

Further advancing the field, [17] examines a linear network architecture for LoRa nodes, arranged sequentially for multi-hop communication. This configuration aims to enhance network reliability and coverage. The study investigates various optimization techniques, including routing protocols and retransmission strategies, providing a robust framework for improving network performance. While the study's contribution to network reliability is commendable, a key drawback is the protocol's limitation to linear networks, which restricts its applicability in more complex network topologies.

Another study [19] presents a multi-hop LoRa protocol focused on minimizing communication latency. This protocol aims to improve responsiveness and efficiency in LoRa networks through optimized routing algorithms and adaptive data rate adjustments. The protocol's ability to reduce latency is highly beneficial for real-time communication. However, a significant limitation is that it does not address energy consumption, which is crucial for large-scale, battery-powered IoT deployments.

In [21], a multi-hop LoRa network with pipelined transmission capability is proposed to improve communication efficiency. This approach demonstrates substantial improvements in throughput, latency, and bandwidth optimization. Its potential to enhance overall network performance is noteworthy, yet a major limitation is that the protocol fails to consider energy consumption, a critical aspect in large-scale IoT networks.

Similarly, the study in [22] integrates time-slotting into LoRaWAN to reduce latency and improve predictability in industrial IoT applications. By allocating specific time intervals for communication, time-slotting improves synchronization. This contribution is valuable for industrial IoT applications where low latency is essential. However, the protocol's failure to address energy consumption could undermine its effectiveness in long-term IoT network operation.

The study in [23] focuses on real-time communication within dynamic LoRa networks, utilizing multi-hop architecture to improve flexibility and network coverage. Its focus on adaptability to changing network conditions makes it a useful solution in dynamic environments. However, its primary focus on industrial applications and its energy demands limit its broader applicability.

A different approach, presented in [26], proposes Multi-LoRa, a multi-radio, multi-hop LoRa architecture designed to improve coverage and service for large-scale rural IoT deployments. The hardware prototype demonstrated a 60% reduction in delay and a 2.9% decrease in packet loss. This approach is a notable improvement in reducing delay and enhancing service in rural areas. However, the increased complexity of the architecture leads to higher energy consumption, which may limit its feasibility for widespread deployments.

The MQ-LoRa protocol [28] introduces a multi-hop protocol for QoS-aware LoRa networks. By using deep reinforcement learning to optimize transmission parameters and employing a hybrid cluster-root rotated tree topology for routing, the protocol demonstrates a promising approach to enhancing network performance. Its positive impact on energy efficiency and packet reception makes it a significant contribution to QoS-aware communication in IoT networks. However, its complexity, particularly due to the deep reinforcement learning approach, can lead to increased latency and energy consumption, limiting its scalability in large networks.

The MauMe protocol, discussed in [29], enables multi-hop communication through an Epidemic Delay Tolerant Network messaging protocol using controlled flooding. Its ability to ensure reliable packet delivery in networks with reduced connectivity is impressive. However, the protocol's flooding mechanism may lead to inefficiencies in energy consumption and latency, especially in large-scale networks where these factors are critical.

Lastly, In [30], MRT-LoRa is introduced as a protocol for real-time data communication in Industrial Internet of Things (IIoT) environments. It optimizes long-range communication by reducing the time-on-air per hop and minimizing duty cycle impact. The protocol's contribution to optimizing communication in large-scale industrial settings is significant. However, its emphasis on real-time data flows leaves out energy consumption considerations, which may be critical in other IoT environments.

One of the key contributions of the protocols presented in this study is their focus on addressing the challenges of latency, energy efficiency, and scalability in LoRa networks, while enabling the easy addition of new nodes without disrupting the ongoing operation of the network. Unlike previous studies that often overlook the balance between latency and energy consumption, the proposed protocols are designed to optimize both aspects. By minimizing latency through efficient routing and transmission policies, these protocols ensure timely communication in real-time applications. At the same time, they incorporate energy-saving mechanisms such as duty cycle optimization and low-power modes to extend the lifetime of battery-powered devices, which is crucial in large-scale IoT deployments. Furthermore, the scalability of these protocols is enhanced by their ability to seamlessly integrate new nodes into the network without causing significant disruptions. This is achieved through dynamic and adaptive routing mechanisms that allow the network to adjust to the addition of new devices, ensuring that the network maintains its performance and reliability even as it expands. This scalability, combined with the ability to optimize both energy consumption and latency, represents a significant step forward compared to previous studies, which often focus on one or two of these aspects without providing an integrated solution for large, growing networks.

3 Low Latency and Energy Efficient Multi-hop Routing Protocol

3.1 LoRa Propagation Model

The path loss equation used in this simulation is based on the macro cell propagation model from reference [31]. This model is adapted to the LoRa channel conditions in urban and suburban scenarios outside high-rise centers, where buildings are relatively homogeneous in height. The parameters in Equation (1), such as the constants 80 and 40, were directly adopted from reference [31], where empirical studies have determined these values based on specific propagation characteristics for urban and suburban areas

$$PL(d) = 80|_{dB} + 40(1 - 0.004h|_m) \log_{10} d|_{km} - 18 \log_{10} h|_m + 21 \log_{10} f|_{MHz} \quad (1)$$

where d is the communication distance between transmitter and receiver in kilometres, h is the antenna height of the receiver in meters, f is the carrier frequency in megahertz.

Some parameters, such as the constants and coefficients in Equation (1), were fine-tuned based on preliminary simulation results to better align with the frequency and antenna height commonly used in the simulated scenarios. If h is set in 2 meters, the path loss can be simplified as follows:

$$PL(d) = 74.58 + 39.68 + \log_{10} d|_{km} + 21 \log_{10} f|_{MHz} \quad (2)$$

The received power at distance d , $P_{rx}(d)$ is computed as follows:

$$P_{rx}(d) = P_{tx} - PL(d) \quad (3)$$

where P_{tx} represents the transmission power, typically measured in dBm and $PL(d)$ denotes the path loss at distance d , measured in dB. The received power $P_{rx}(d)$ is thus calculated by subtracting the path loss $PL(d)$ from the transmission power P_{tx} . This relationship shows that as the distance d between transmitter and receiver increases, the path loss $PL(d)$ generally increases, resulting in a lower received power $P_{rx}(d)$.

Assuming that if the received power P_{rx} is equal to or greater than the receiver's receiving sensitivity, S , the LoRa signal can be well demodulated. Additionally, the lowest received power P_{rxmin} must be more than $S + \text{link margin}$ in order for the signal to be successfully demodulated. Equations

(4) and (5) can be used to obtain the minimal received power P_{rxmin} and the receiving sensitivity of the receiver (S) [32].

$$S = -174 + \log_{10} BW + NF + SNR \quad (4)$$

where SNR denotes the signal-to-noise ratio required by the underlying modulation technique, BW is the bandwidth of receiver, NF is the noise figure of receiver, and is set for a given hardware implementation.

$$P_{rxmin} = S + linkmargin \quad (5)$$

Thus, the maximum communication distance d_{max} can be calculated as follows:

$$d_{max} = 10^{((P_{tx} - P_{rxmin} - 20 \log_{10} f - 78.58) / 39.68)} \quad (6)$$

3.2 LoRa Energy Consumption Model

This study aims to analyze the energy consumption of LoRa devices across various operating modes to optimize power efficiency in IoT applications. The SX1276 LoRa device was selected for its popularity, compatibility with various IoT applications, and its operating frequency range of 920–923 MHz, which complies with the frequency regulations in Indonesia and falls within the SX1276's specifications. Four operating modes are considered based on their current consumption characteristics, as shown in Table 1. This approach enables an accurate calculation of LoRa energy consumption in transmit, receive, standby, and sleep modes by taking into account the current consumption characteristics of each mode as well as the active time duration based on time on air (ToA) values. To compute the energy consumption in receive and transmit modes, it is necessary to consider the (ToA) or packet duration (T_{packet}) [32], as shown in the following equation.

$$T_{packet} = T_{preamble} + \eta_{pldSym} + T_{sym} \quad (7)$$

where Equations (8), and (9) represent the duration of the preamble and symbol. Equation (10) is the quantity of payload and header symbols.

$$T_{preamble} = (\eta_{preamble} + 4.25) \times T_{sym} \quad (8)$$

$$T_{sym} = \frac{2^{SF}}{BW} \quad (9)$$

$$\eta_{pldSym} = 8 + \max(\text{ceil}(\frac{8PS + 28 + 16 - 20H}{4(SF - 2DE)}))(CR + 4), 0) \quad (10)$$

Tx Energy Consumption: The SX1276 LoRa device has two TX power selection configurations, each connected to different output pins. To select the appropriate configuration, both hardware and software settings must be adjusted. These configurations are as follows [33]:

- RFOP_HF/LF Pin : This is a low-power amplifier with an output power of +7 or +13 dBm where RFOP_HF is for band 1 and RFOP_LF is for bands 2 & 3.
- PA_BOOST Pin : This provides an output RF power of +17 dBm or, in High Power Operation (HPO) mode, +20 dBm.

In our simulation, we adopted RF-LORA-195-SO module, which integrates Semtech's SX1276 LoRa transceiver, offering a reliable and efficient solution for LoRa-IoT applications. This module was specially created a model in the NS-3 LoRa module due to its ability to provide a direct output to the PA_BOOST pin, which is crucial for achieving the higher transmission power and long-range coverage required in our simulation. The specific parameters of the SX1276 LoRa transceiver are detailed in Table 1. Using Equation (7) and the values provided in Table 1, the energy consumption in transmit mode is calculated using Equation (11) as follows.

$$E_{tx} = V_D \times I_{tx} \times T_{packet} \quad (11)$$

where V_D is the voltage used by the device during transmit mode. I_{tx} is the current consumed by the device in transmit mode. T_{packet} is the packet duration, which is the time required for transmitting data.

Rx Energy Consumption: The LNA (Low Noise Amplifier) boost option on the SX1276 enhances performance in RX mode by improving the signal-to-noise ratio, allowing for better reception of weak signals, but it consumes more current. The values for both setups are provided in Table 1. Therefore, the energy consumption in receive mode can be calculated using Equation (12), as follows.

$$E_{rx} = V_D \times I_{rx} \times T_{packet} \quad (12)$$

where I_{rx} is the current consumption in receive mode

Standby Current Consumption: Refers to the power consumption that occurs when the device is in standby mode, where it is not actively transmitting or receiving data but still consumes power to maintain certain functions, such as listening for signals or staying ready. Thus, the energy consumption in standby mode can be determined using Equation (13), as shown below.

$$E_{sb} = V_D \times I_{sb} \times T_{standby} \quad (13)$$

where I_{sb} is the current consumption in standby mode

Sleep Current Consumption: This refers to the power consumed by the device when it is in sleep mode, where it is completely inactive and not participating in any transmission or reception of data. In this mode, the device minimizes its energy usage by shutting down most of its components, but it still consumes a small amount of power to maintain essential functions, such as waking up periodically to check for incoming signals or data. Therefore, the energy consumption in sleep mode can be calculated using Equation (14), as illustrated below.

$$E_{sleep} = V_D \times I_{sl} \times T_{sleep} \quad (14)$$

where I_{sl} is the current consumption in sleep mode and T_{sleep} is the duration in sleep mode

In Table 1, the current consumption of the SX1276 LoRa, produced by Semtech, is used as a reference from practical experience for calculating energy consumption in Tx, Rx, standby, and sleep modes. This data provides a foundational understanding of power consumption that can be applied generally to LoRa-based systems. However, the method used to calculate energy consumption can also be applied to LoRa devices from other manufacturers. While each LoRa chip from different manufacturers may have slightly different power consumption values, the basic principles of measurement and calculation still apply to other devices with adjustments made according to the relevant technical data.

Table 1: Current Consumption of SX1276 LoRa [33]

Description	Conditions	Typ(mA)
Sleep mode	-	0.2×10^{-3}
Standby mode	-	1.6
Receive mode	Band 1, without LNA Boost	10.8
	Band 1, with LNA Boost	11.5
	Band 2 & 3	12.5
Transmit mode on PA_BOOST	RFOP=+20 dBm	120
	RFOP=+17 dBm	87
Transmit mode on RFO_LF/HP pin	RFOP=+13 dbm	29
	RFOP=+7 dBm	20

3.3 Design of Proposed Multi-hop Routing Protocol

3.3.1 Network Establishment

To establish a multi-hop network, the routing protocol uses four operations, two operations conducted by the parent node and two operations conducted by the child node, where each operation is completed at one timeslot (TS). The two operations of the parent node are OFR (offer) and ACK (acknowledge) and the two operations of the child node are JOIN (join request) and NOTF (notify). Thus, each cycle needs four timeslot (TS) as shown in Figure 2.

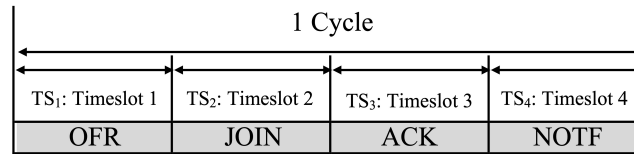


Figure 2: Four timeslots in each cycle in the network establishment

To create a link between a parent node and a child node, In TS₁, the parent node first transmits a packet of OFR(T_{id}, R_n) where T_{id} is the node ID of the transmitter as parent and R_n is the n^{th} ring number to all reachable children nodes in the R_n+1 ring. Each reachable child node tries to receive an OFR packet from the parent node. Furthermore, in the next cycle TS₂, the child node sends a JOIN(T_{id}, R_{id}, R_n, C_u) packet where T_{id} is the transmitter's ID, R_{id} is the receiver's ID, and C_u is a channel-timeslot list used by its neighbors to the parent node. The parent uses the C_u to give a time slot and a channel that won't collide with any of its close neighbors.

After sending the OFR packet, the parent node receives a JOIN packet from a child node and allocates a collision-free channel and a timeslot which are not used in the used cell list C_u for being sent to the child node. Furthermore, In TS₃, the parent node sends a packet of ACK($T_{id}, R_{id}, R_n, C_h, Ts$) to the child node, where C_h and Ts are the allocation cell (channel and timeslot) which is used to communicate between the parent and the child node.

The parent node is added to the child node's parent list (PL) when the child node receives an ACK packet from the parent node. Lastly, in TS₄ it broadcasts a packet of NOTF($T_{id}, R_{id}, R_n, C_h, Ts$) to notify its cell allocation to its neighbors.

In TS₁ and TS₂, a collision may happen when the child nodes receive an OFR packet and send a JOIN packet simultaneously to the parent, as indicated In Figure 3. To avoid the collision, a collision-prevention mechanism is proposed, which is explained in the next subsection.

3.3.2 Packet Collision Prevention

In LoRa real, packet collision can be avoided using a channel activity detection (CAD) mechanism [19]. Each node sends a packet, and other nodes acting as receivers can detect the packet in the air. To detect the packet, the node needs time T_{CAD} , which is equal to two times T_{sym} and depends on the spreading factor. Therefore, to prevent packet collisions, each node can send a packet after a random

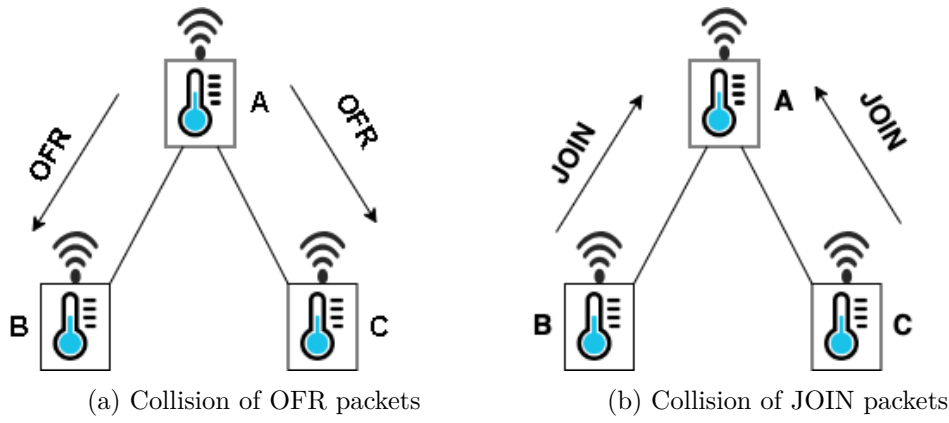


Figure 3: Packet collision in the network establishment

delay time of dt , where $dt = r \times T_{CAD}$ and r is a random number determined by the contention window size.

In the context of LoRa simulation, a packet collision may occur when two or more nodes use the same channel or spreading factor and send packets simultaneously. By keeping track of every event, it is possible to identify the simultaneous use of a channel or spreading factor. Data regarding the ToA time, spreading factor, frequency, packet, and received power are all included in each event. The node recognises a packet as destroyed if it detects two or more events with the same spreading factor or frequency throughout the ToA timeframe. Therefore, a node can send a packet after the ToA delay time in order to avoid the packet collision.

3.3.3 Channel and Timeslot Assignment

A parent node assigns a channel and timeslot using Algorithm 1 to a child node after receiving an JOIN packet from the child node and transmitting an ACK packet to the child node. Furthermore, the parent node updates the children list and the child node updates its parent. The parent node examines the list of channels and timeslots that have been used by other nodes to ensure that the channel and timeslot it assigns to its child are collision-free.

The channels are split by the number of branches in order to reduce the usage of the eight limited channels. The channel number is decreased by 1 for the node in the subsequent ring. For instance, channel 0 is allocated to all nodes in branch and ring 1. Furthermore, the rings 2, 3, 4, and so on are given the channels 1, 2, 3 and so forth. On the other hand, each node allocates a timeslot with a difference of 1 to its other offspring to reduce the usage of that timeslot. The parent node gathers data from all of its child nodes to be relayed to its parent to reduce the number of times that data must be transmitted again.

Algorithm 1 Channel and timeslot assignment

Input: number of channels: nch ; number of rings: nr ; node type: tp ; Parent: P_L ; Vector children: $C_i, \forall i \in C$; Vector neighbour: $N_j, \forall j \in N$

Output: channel: ch ; timeslot: ts

Initialization

```

1:  $ch \leftarrow 0$ 
2: if  $tp = GW$  then
3:    $ts \leftarrow nr \times 2$ 
4:    $ch \leftarrow ch + 1$ 
5:   if  $ch = nch$  then
6:      $ch \leftarrow 0$ 
7:   end if
8: else
9:    $ts \leftarrow P_L.ts - 1$ 
10:   $ch \leftarrow P_L.ch$ 
11: end if
12: for  $j \in N$  do
13:   if  $N_j.ts = ts$  then
14:      $ts \leftarrow ts - 1$ 
15:   else if  $N_j.ch = ch$  then
16:      $ch \leftarrow ch + 1$ 
17:     if  $ch = nch$  then
18:        $ch \leftarrow 0$ 
19:     end if
20:   end if
21: end for
22: for  $i \in C$  do
23:   if  $C_i.ts = ts$  then
24:      $ts \leftarrow ts - 1$ 
25:   end if
26: end for

```

3.3.4 Mechanism for Adding a New Node

When a new node wish join in the network, it initializes itself with default settings and LoRa parameters. The new node sends a join request (JOIN packet) to all neighbouring nodes that serve as a potential parent or relay node. The potential parent nodes evaluate the join request based on factors like the smallest number of children, proximity, and packet aggregation size. If accepted, the parent node sends an acknowledgement (ACK packet) to the new node by sending a timeslot and channel assignment to identify the least congested or occupied channel within its communication range. Furthermore, the new node confirms its addition to the neighbors by sending a NOTF packet. Finally, the parent node updates its children list, the new node adds its parent to the parent list, and the neighboring nodes update its used cell list C_u .

For instance, in Figure 4, nodes A, B, C, D, or F can be chosen as parents of the node G. Because node C has the smallest number of children and is nearest to the node G, node G choose it as its parent. Therefore, the latency of node G to node A is lowest because node G only has a hop count of two. Because a smaller packet size is crucial for data aggregation, parent choice plays a significant role in reducing packet size [34]. Moreover, to avoid exceeding the packet aggregation size and minimizing the end-to-end latency, node G rejects node B as its parent but it chooses node C.

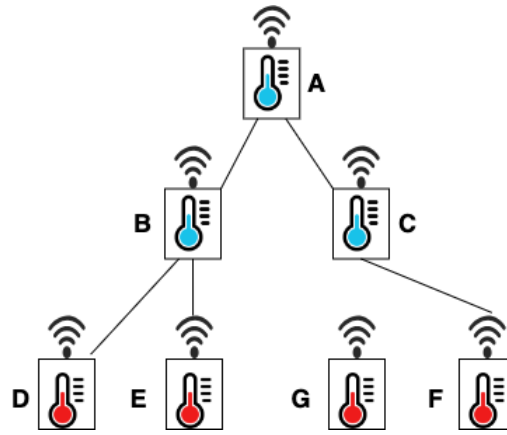


Figure 4: Mechanism for Adding a New Node

4 Performance Evaluation

The simulation setup and the simulation results are covered in detail in the discussion of the performance evaluation. First, the simulation setup explains how to build nodes that are deployed over a wide area to construct a multi-hop network. Additionally, it describes how a node in the outer ring of the built-in network is included. Second, the simulation results show how to evaluate performance by calculating the total energy used to build a multi-hop network and network latency, which is the time it takes for data to transmit from nodes in the outer ring to the gateway.

4.1 Simulation Setup

For simulation, a network simulator Version 3 (NS-3) and NS-3 LoRa module [35] are used to construct the multi-hop networks and to calculate the performance evaluation. Besides, the wireless communication device used is LoRa SX1276 with parameter setting as shown in Table 2. According to Indonesian regulation, which is decided by the Minister of Communication and Informatics, the uplink frequency is fixed at 920-923 MHz, which is divided into 8 channels. The results presented in this study are based on these simulations, and the use of NS-3, with the addition of several models from the LoRa module such as the LoRa propagation model, LoRa energy consumption model, and LoRa multi-hop routing model, along with their respective derivative models, ensures a high degree of realism and accuracy in evaluating the performance of the network under various conditions. Although these results have not been validated experimentally yet, the simulation setup closely follows real-world configurations, providing a strong foundation for the findings.

Table 2: LoRa Parameter Setting

Parameter	Value
Bandwidth (kbps)	125
Frequency Channel (MHz):	
Channel 1 – 4 (Ch_1 - Ch_4)	920.2 – 920.8
Channel 5 – 8 (Ch_5 - Ch_8)	921.2 – 921.8
Power Transmission	7, 14, 17 dBm
Spreading Factor	7
Number of Preamble Symbols	8
Coding Rate	4/8
Header Disabled	0
Cyclic Redundancy Check Enabled	0
Low Data Rate Optimization Enabled	0

4.2 Network Establishment

For network establishment simulation, 93 nodes denoted by a circle are distributed in a wide square area of 60 x 60 km² and are deployed in 5 rings. In addition, a gateway (GW) marked by a red triangle is located at the center, as shown in Figure 5. The simulation is set using the network structure parameter as shown in Table 3.

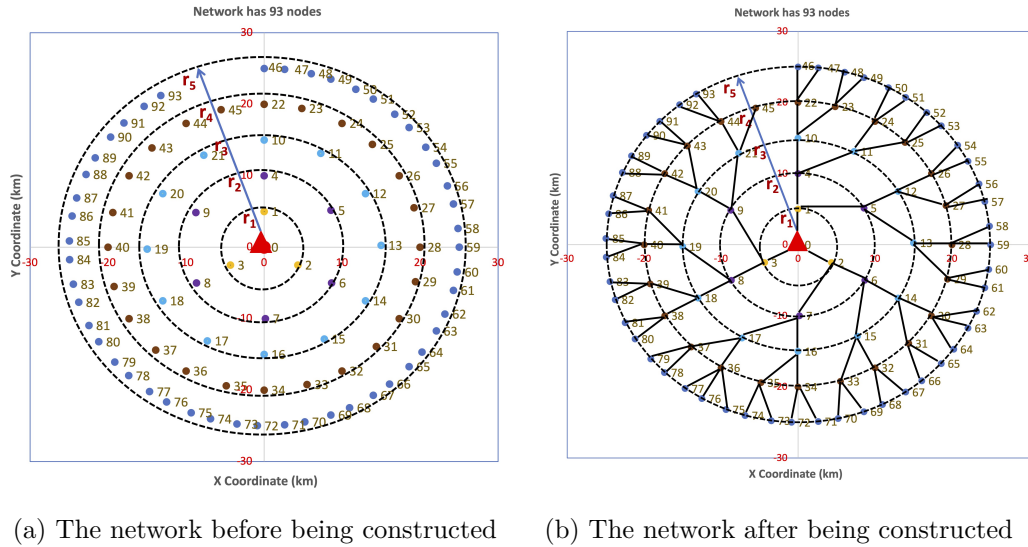


Figure 5: Network establishment

Table 3: Network structure parameter for network establishment

Parameter	Value
Number of branches	3
Number of rings	5
Number of nodes	192
Distance between rings	5 km

By applying Algorithm 1, a multi-hop network construction can be created, as illustrated in Figure 5. With the exception of the outer ring, every node in every ring creates a link by having two children nodes. However, node 30 and node 36 are two of the ring 4's two nodes that have three nodes. In this instance, node 30 can respond to node 64 more quickly than node 31. Similar circumstances apply to node 77, which receives a response from node 36 before node 37. Furthermore, to avoid data transmission collisions, each node in each branch and ring will have a channel and time slot that are set using Algorithm 1 with the results as shown in Table 4. Channels Ch_0 , Ch_1 , Ch_2 , and Ch_3 are used, respectively, by the nodes connected in branches 1 through 3 that are situated in rings of 1 through 3. On the other hand, the nodes in rings 4 and 5, use channels Ch_2 , Ch_3 , Ch_4 , and Ch_5 . Furthermore, the utilization of the various timeslots was changed, and 10 timeslots were required. The two children nodes of a parent node use timeslots 1 and 2 for nodes put on the outer ring.

Table 4: Channel and time slot after the network establishment

Branch	Ring														
	Node ID	Ch	Time Slot	Node ID	Ch	Time Slot	Node ID	Ch	Time Slot	Node ID	Ch	Time Slot	Node ID	Ch	Time Slot
1	1	0	10	4,5	0	7-6	10-13	1	6-5	22-29	2	4-3	46-61	3	2-1
2	2	1	9	6,7	1	7-6	14-17	2	6-5	30-37	3	4-3	62-78	4	2-1
3	3	2	8	8,9	2	7-6	18-21	3	6-5	38-45	4	4-3	79-93	5	2-1

4.2.1 New Node Adding

Several nodes in a ring request to join the network after the network has been established. The network uses the node-adding mechanism in subsection 3.3.4 to add any node in the ring. For instance, Figure 6a shows nodes 94 and 95 that will be added to the network. As a result, the network illustrated in Figure 6b shows the two nodes, 94 and 95, connected to node 45 in ring 4. The successful addition of new nodes to the network without disrupting the ongoing network operations using this node-adding mechanism aligns with the approach used by [19], although applied to a different network architecture.

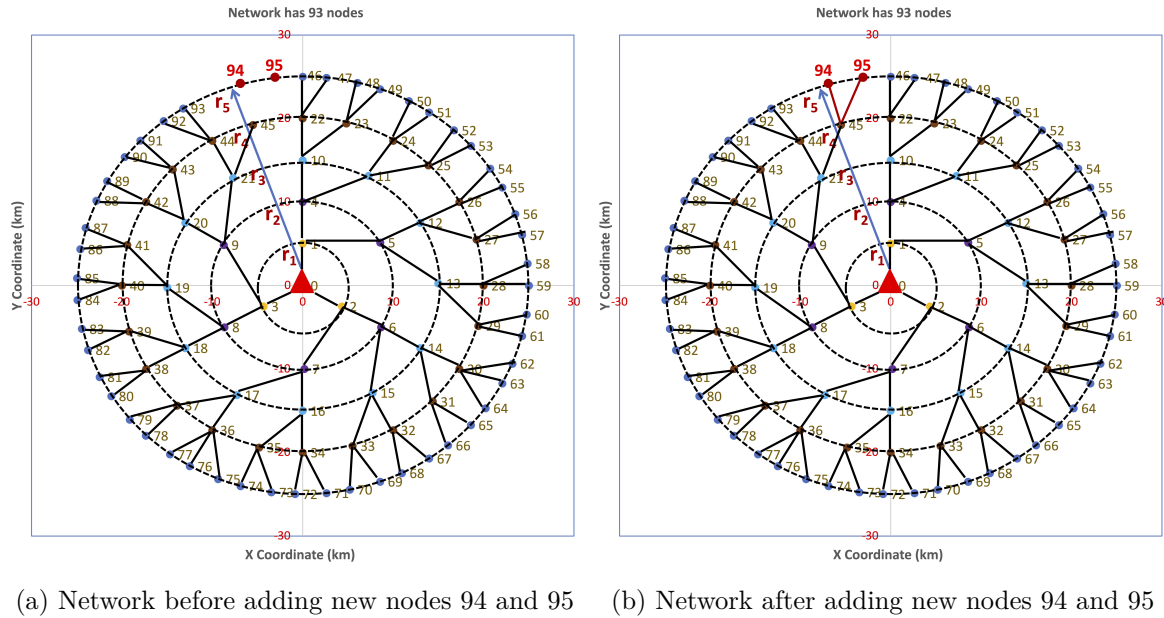


Figure 6: Adding new nodes in the network

4.3 Simulation Results

4.3.1 Energy Consumption of Network Construction

Energy consumed by the network construction is evaluated in five network structure scenarios by using Table 5. The evaluation results of five scenarios demonstrate that the overall energy consumption of the network construction increases along with the increase of total involved nodes in the network. However, as depicted in Figure 7, the energy consumption is kept comparatively low. For instance, the amount of energy consumption for 3270 nodes is 31.01 joule. These are because of the network construction mechanism which uses four simple operations: offer, interest, confirm, and announce. Two operations of offer and interest are conducted by the parent node, whereas two other operations are conducted by the child node.

Table 5: Networks Structure Parameter

Parameter	Scenario				
	1	2	3	4	5
Number of rings	3	4	5	6	7
Number of branches	3	3	3	3	3
Number of nodes	39	120	363	1092	3279

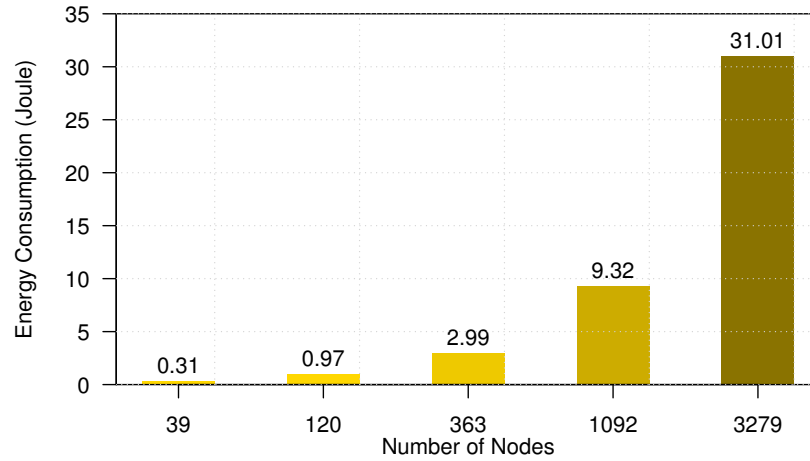


Figure 7: Total energy consumption of the network construction

The comparison between our research and the study by Chen et al. [36], highlights key differences in energy efficiency and system configuration. In our study, a single static gateway achieved an energy consumption of 31.01 joules for 3,279 nodes over a 25 km² area. Conversely, the study by Chen et al. recorded an energy consumption of approximately 42 joules for 3,000 nodes in the same area using three mobile gateways deployed via drones.

The lower energy consumption in our approach demonstrates the efficiency of utilizing a static gateway in a controlled environment, optimizing resource use while maintaining extensive coverage. In contrast, the higher energy consumption observed in Chen et al.'s study can be attributed to the additional power required to operate and manage multiple mobile gateways via drones, which introduce dynamic positioning and increased operational complexity.

This comparison validates the efficiency of our methodology, particularly in scenarios where static infrastructure is feasible and cost constraints are critical. While the mobile gateway approach offers flexibility and potentially improved connectivity in challenging terrains, the simplicity and lower energy demands of our static gateway design underscore its practical advantages for large-scale deployments in stable environments. This supports the reliability of our findings and their applicability in energy-sensitive IoT networks.

4.3.2 Low Latency Network

Network latency is evaluated by calculating the delay for all nodes located in the outer ring of the GW. Each node undergoes five hops to reach the GW. Given that the distance between rings is set at 5 km, the average path distance for each node in the outer ring is 32.76 km to the GW. The delay is calculated using the distance (d_{max}) from Equation (6), based on the macro cell propagation model for path loss with shadowing to represent wireless channels in built-up and densely populated areas. The maximum, minimum, and average delays for the outer nodes (node IDs: 46-93) are presented in Table 6.

These delay values are closely related to the structural characteristics of the network. For every branch of the network, the delay pattern in Figure 8 and the distance pattern in Figure 9 are identical. The node selection mechanism determines both the distance and delay patterns, with nodes aligned with the GW having shorter distances compared to those positioned at specific slope angles from the GW. As a result, the delay pattern follows the distance pattern.

This correlation between delay and distance is further validated by the total delay values. The total delay, with a maximum of 113.28 seconds and a minimum of 85.32 seconds as listed in Table 6, represents the delay experienced by the outermost nodes to the GW through multiple hops. The difference of 29.76 seconds between the maximum and minimum delay remains within the tolerable range for multi-hop communication in IoT networks. Consequently, despite variations in delay between

the outer nodes, the delay pattern aligns with the distance pattern established by the node selection mechanism, where nodes positioned directly toward the GW experience shorter delays compared to those located at an angle.

The delay performance comparison between our study and MRT-LoRa [30] shows significant differences. In the MRT-LoRa study, which uses a 3-hop network, the cumulative percentage distribution of delays increases linearly from 0 to 95% between 0 and 14 seconds. However, delays between 14 and 30 seconds only increase by 5%, indicating a relatively stable performance despite some delay variation. This pattern suggests that MRT-LoRa is optimized to maintain low delays over a smaller network with fewer hops.

In contrast, our study uses a 5-hop network with an average distance of 32.76 km between outer nodes and the gateway (GW), resulting in much higher delay values, ranging from a minimum of 83.52 seconds to a maximum of 113.28 seconds. The increased number of hops and longer distances naturally lead to higher delays. The greater delay variation in our study compared to MRT-LoRa can be attributed to the additional hops, which introduce more latency due to processing time, transmission, and re-transmissions involved at each hop.

While the MRT-LoRa system shows relatively stable delays within a 30-second range for its 3-hop configuration, our system with 5 hops shows considerably higher delay values, as expected from a larger network setup. These results indicate that our network prioritizes broader coverage, while MRT-LoRa focuses on minimizing delays in a smaller, more compact network. The higher delays in our system reflect the trade-off between extended range and real-time performance, whereas MRT-LoRa demonstrates an efficient balance of low delays for real-time communication within a more compact network.

Table 6: Delay of the network

	Delay (second)					Total
	Ring					
	4	3	2	1	GW	
Max	18.42	22.49	26.93	28.60	16.68	113.28
Min	16.68	16.68	16.68	16.68	16.68	83.52
Average	17.36	19.06	21.03	21.89	16.68	96.18

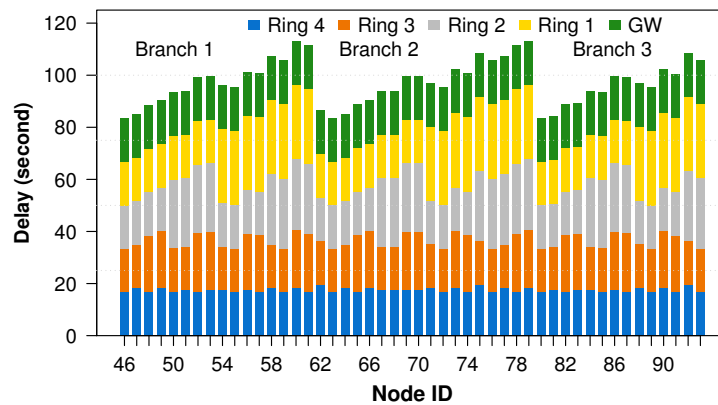


Figure 8: Delay of the network in each branch and ring

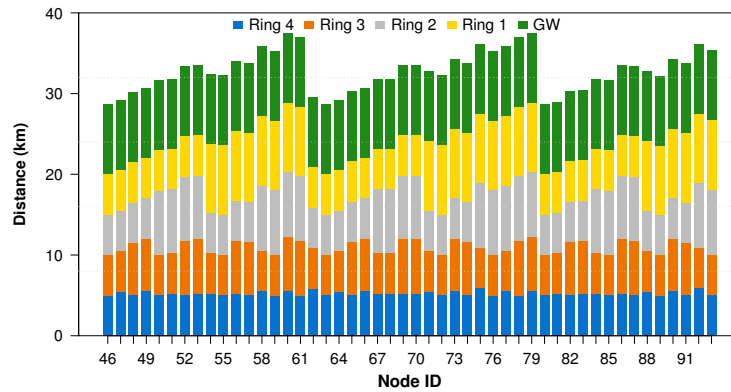


Figure 9: Path distance between nodes in the outer ring to the gateway

5 Conclusion

In this study, we proposed a multi-hop routing protocol specifically designed for IoT networks to achieve low latency, energy efficiency, and flexible scalability, enabling the seamless integration of new nodes. The protocol's performance was evaluated across five-hop scenarios, with an average distance of 32.76 km. The energy consumption ranged from 0.31 joules for 39 nodes to 31.01 joules for 3,279 nodes, demonstrating a direct correlation between network scale and energy consumption. This underscores the importance of energy efficiency, particularly in large-scale LoRa networks, when designing sustainable IoT systems.

The delay analysis further demonstrates that the delay pattern closely mirrors the distance pattern, with nodes positioned along the Gateway (GW) line experiencing shorter distances and lower delays compared to nodes placed at an angle to the GW. Additionally, the delay pattern aligns with the spacing between network rings, indicating that the node selection mechanism plays a key role in maintaining a consistent and predictable delay distribution across the network.

Additionally, the study reveals that the network successfully integrates new nodes through an effective node-adding mechanism, allowing for smooth integration into existing ring structures. This mechanism not only supports the protocol's scalability but also reinforces its capacity to expand without disrupting ongoing communication, ensuring continuous network performance as new nodes are added.

The proposed protocol is particularly well-suited for LoRa communication technology, which is characterized by longer packet transmission times compared to other wireless sensor network (WSN) technologies. By preventing data packet collisions with neighboring nodes, the protocol ensures reliable data transmission. Simulations demonstrate that the protocol maintains low latency, conserves energy, and enables seamless node integration, confirming its efficiency and scalability.

While the study demonstrates the protocol's strong performance in reducing latency, conserving energy, and offering flexibility in adding nodes, it also suggests areas for future research. Given that LoRa technology is optimized for longer packet transmission times, there may be constraints in specific use cases. Therefore, further research should focus on enhancing the protocol's robustness, considering diverse network conditions, real-world deployment challenges, and ensuring its practical applicability across a broad range of IoT environments.

Acknowledgement

The authors would like to express their sincere gratitude to the Ministry of Education, Culture, Research, and Technology of Indonesia for their financial support through the national competitive basic research scheme, under Contract Number: 134/E5/PG.02,00,PL/2023. This support has been essential for the successful completion of this research.

References

- [1] M. S. Philip and P. Singh, *An energy efficient algorithm for sustainable monitoring of water quality in smart cities*, *Sustain. Comput. Informatics Syst.*, vol. 35, p. 100768, 2022.
- [2] B. Miles, E.-B. Bourennane, S. Boucherkha, and S. Chikhi, *A study of LoRaWAN protocol performance for IoT applications in smart agriculture*, *Comput. Commun.*, vol. 164, pp. 148–157, 2020.
- [3] A. Parihar, J. B. Prajapati, B. G. Prajapati, B. Trambadiya, A. Thakkar, and P. Engineer, *Role of IOT in healthcare: Applications, security & privacy concerns*, *Intell. Pharm.*, 2024.
- [4] V. Kamatchi Sundari, J. Nithyashri, S. Kuzhaloli, J. Subburaj, P. Vijayakumar, and P. Subha Hency Jose, *Comparison analysis of IoT based industrial automation and improvement of different processes – review*, *Mater. Today Proc.*, vol. 45, pp. 2595–2598, 2021.
- [5] B. S. Chaudhari, M. Zennaro, and S. Borkar, *LPWAN Technologies: Emerging Application Characteristics, Requirements, and Design Considerations*, *Future Internet*, vol. 12, no. 3, 2020.
- [6] J. R. Cotrim and J. H. Kleinschmidt, *LoRaWAN Mesh Networks: A Review and Classification of Multihop Communication*, *Sensors (Basel)*, vol. 20, 2020.
- [7] J. Dias and A. Grilo, *LoRaWAN multi-hop uplink extension*, *Procedia Comput. Sci.*, vol. 130, pp. 424–431, 2018.
- [8] M. Anedda, C. Desogus, M. Murroni, D. D. Giusto, and G.-M. Muntean, *An Energy-efficient Solution for Multi-Hop Communications in Low Power Wide Area Networks*, in 2018 IEEE International Symposium on Broadband Multimedia Systems and Broadcasting (BMSB), 2018, pp. 1–5.
- [9] M. H. Dwijaksara, W. S. Jeon, and D. G. Jeong, *Multihop Gateway-to-Gateway Communication Protocol for LoRa Networks*, in 2019 IEEE International Conference on Industrial Technology (ICIT), 2019, pp. 949–954.
- [10] W. Zhou, Z. Tong, Z. Y. Dong, and Y. Wang, *LoRa-Hybrid: A LoRaWAN Based Multihop Solution for Regional Microgrid*, in 2019 IEEE 4th International Conference on Computer and Communication Systems (ICCCS), 2019, pp. 650–654.
- [11] J. Dias and A. Grilo, *Multi-hop LoRaWAN uplink extension: specification and prototype implementation*, *J. Ambient Intell. Humaniz. Comput.*, vol. 11, no. 3, pp. 945–959, 2020.
- [12] M. S. Aslam et al., *Exploring Multi-Hop LoRa for Green Smart Cities*, *IEEE Netw.*, vol. 34, no. 2, pp. 225–231, 2020.
- [13] M. Kim and J. Jang, *A Study on Implementation of Multi-hop Network for LoRaWAN Communication*, in 2020 International Conference on Information Networking (ICOIN), 2020, pp. 553–555.
- [14] L. Feng, H. Yu, and M. Jia, *A Hierarchy-Based Dynamic Routing Protocol for LoRa Mesh Networks*, in 2023 IEEE International Symposium on Broadband Multimedia Systems and Broadcasting (BMSB), 2023, pp. 1–6.
- [15] C.-H. Liao, G. Zhu, D. Kuwabara, M. Suzuki, and H. Morikawa, *Multi-Hop LoRa Networks Enabled by Concurrent Transmission*, *IEEE Access*, vol. 5, pp. 21430–21446, 2017.
- [16] B. Sartori, S. Thielemans, M. Bezunartea, A. Braeken, and K. Steenhaut, *Enabling RPL multihop communications based on LoRa*, in International Conference on Wireless and Mobile Computing, Networking and Communications, 2017, vol. 2017-Octob.

- [17] C. T. Duong and M. K. Kim, *Reliable multi-hop linear network based on LoRa*, Int. J. Control Autom., vol. 11, pp. 143–154, 2018.
- [18] A. Abrardo, A. Fort, E. Landi, M. Mugnaini, E. Panzardi, and A. Pozzebon, *Black Powder Flow Monitoring in Pipelines by Means of Multi-Hop LoRa Networks*, in 2019 IEEE International Workshop on Metrology for Industry 4.0 and IoT, MetroInd 4.0 and IoT 2019 - Proceedings, 2019, pp. 312–316.
- [19] D. L. Mai and M. K. Kim, *Multi-hop LoRa network protocol with minimized latency*, Energies, vol. 16, no. 3, 2020.
- [20] H. P. Tran, W.-S. Jung, T. Yoon, D.-S. Yoo, and H. Oh, *A Two-Hop Real-Time LoRa Protocol for Industrial Monitoring and Control Systems*, IEEE Access, vol. 8, pp. 126239–126252, 2020.
- [21] D. L. Mai and M. K. Kim, *Multi-hop lora network with pipelined transmission capability*, Lect. Notes Comput. Sci. (including Subser. Lect. Notes Artif. Intell. Lect. Notes Bioinformatics), vol. 12293, pp. 125–135, 2020.
- [22] D. Zorbas, K. Abdelfadeel, P. Kotzanikolaou, and D. Pesch, *TS-LoRa: Time-slotted LoRaWAN for the Industrial Internet of Things*, Comput. Commun., vol. 153, pp. 1–10, 2020.
- [23] H. P. Tran, W.-S. Jung, D.-S. Yoo, and H. Oh, *Design and Implementation of a Multi-Hop Real-Time LoRa Protocol for Dynamic LoRa Networks*, Sensors, vol. 22, no. 9, 2022.
- [24] M. Bezunartea, R. Van Glabbeek, A. Braeken, J. Tiberghien, and K. Steenhaut, *Towards Energy Efficient LoRa Multihop Networks*, in 2019 IEEE International Symposium on Local and Metropolitan Area Networks (LANMAN), pp. 1–3, 2019.
- [25] Y. H. Tehrani, A. Amini, and S. M. Atarodi, *A Tree-Structured LoRa Network for Energy Efficiency*, IEEE Internet of Things J., vol. 8, no. 7, pp. 6002–6011, 2021.
- [26] L. Prade, J. Moraes, E. de Albuquerque, D. Rosário, and C. B. Both, *Multi-radio and multi-hop LoRa communication architecture for large scale IoT deployment*, Comput. Electr. Eng., vol. 102, p. 108242, 2022.
- [27] J. Gu, S.-S. Lee, and H. Kang, *DSME-FOTA: Firmware over-the-air update framework for IEEE 802.15.4 DSME MAC to enable large-scale multi-hop industrial IoT networks*, Internet of Things, vol. 27, p. 101239, 2024.
- [28] M. S. A. Muthanna et al., *Deep reinforcement learning based transmission policy enforcement and multi-hop routing in QoS aware LoRa IoT networks*, Comput. Commun., vol. 183, pp. 33–50, 2022.
- [29] J.-M. Mari and A. Gabillon, *The MauMe network - A LoRa multi-hop collaborative protocol and low-cost implementation example*, Comput. Stand. Interfaces, vol. 86, p. 103733, 2023.
- [30] L. Leonardi, L. Lo Bello, and G. Patti, *MRT-LoRa: A multi-hop real-time communication protocol for industrial IoT applications over LoRa networks*, Comput. Commun., vol. 199, pp. 72–86, 2023.
- [31] 3GPP, *3rd Generation Partnership Project; Technical Specification Group Radio Access Network; Evolved Universal Terrestrial Radio Access (E-UTRA); Radio Frequency (RF) system scenarios (Release 13)*, 36.942, 2016.
- [32] Semtech, *SX1272/3/6/7/8 LoRa Modem Design Guide AN1200.13*, Corporation, Semtech, 2013. [Online]. Available: https://www.semtech.com/uploads/documents/LoraDesignGuide_STD.pdf. [Accessed: 16-Oct-2022].

- [33] Semtech, *WIRELESS & SENSING PRODUCTS, DATASHEET, SX1276/77/78/79 - 137 MHz to 1020 MHz Low Power Long Range Transceiver*, 2020. [Online]. Available: https://semtech.my.salesforce.com/sfc/p/#E0000000JelG/a/2R0000001Rbr/6EfVZUorrpoKFfvaF_Fkpgp5kzjiNyiAbqcpqh9qSjE. [Accessed: 09-Oct-2022].
- [34] Y. Gao, X. Li, J. Li, and Y. Gao, *Distributed and Efficient Minimum-Latency Data Aggregation Scheduling for Multichannel Wireless Sensor Networks*, IEEE Internet Things J., vol. 6, no. 5, pp. 8482–8495, 2019.
- [35] T. Leonard and H. To Thanh, *NS3 LoRa Module*, Free Software Foundation, 2021. [Online]. Available: <https://github.com/drakkar-lig/lora-ns3-module>. [Accessed: 03-May-2023].
- [36] C. Chen, J. Luo, Z. Xu, R. Xiong, D. Shen, and Z. Yin, *Enabling large-scale low-power LoRa data transmission via multiple mobile LoRa gateways*, Comput. Networks, vol. 237, p. 110083, 2023.



Copyright ©2025 by the authors. Licensee Agora University, Oradea, Romania.

This is an open access article distributed under the terms and conditions of the Creative Commons Attribution-NonCommercial 4.0 International License.

Journal's webpage: <http://univagora.ro/jour/index.php/ijccc/>



This journal is a member of, and subscribes to the principles of,
the Committee on Publication Ethics (COPE).

<https://publicationethics.org/members/international-journal-computers-communications-and-control>

Cite this paper as:

Misbahuddin, M.; Iqbal, M.S.; Akbar, LASI. (2025). A Multi-Hop Routing Solution for Low Latency and Energy Efficiency in Large-Scale LoRa IoT, *International Journal of Computers Communications & Control*, 20(3), 6501, 2025.

<https://doi.org/10.15837/ijccc.2025.3.6501>